Particuology 110 (2026) 96–108

Contents lists available at ScienceDirect

Particuology

journal homepage: www.elsevier.com/locate/partic

Feasibility study on use of Arabic gum as alternative to corn starch in bonding self-reducing briquettes made by integrated cycle by-products

Sara Scolari*, Davide Mombelli, Gianluca Dall'Osto, Carlo Mapelli

Politecnico di Milano, Dipartimento di Meccanica, Via La Masa 1, 20156, Milano, Italy

HIGHLIGHTS

- Arabic gum improves fine-particle briquette strength via better densification.
- Coarse-particle briquettes lose impact resistance when bonded with Arabic gum.
- Fine BFS with Arabic gum shows higher reduction degree due to better contact.
- Recycled Arabic gum solution matches natural binder in briquette performance.

GRAPHICAL ABSTRACT

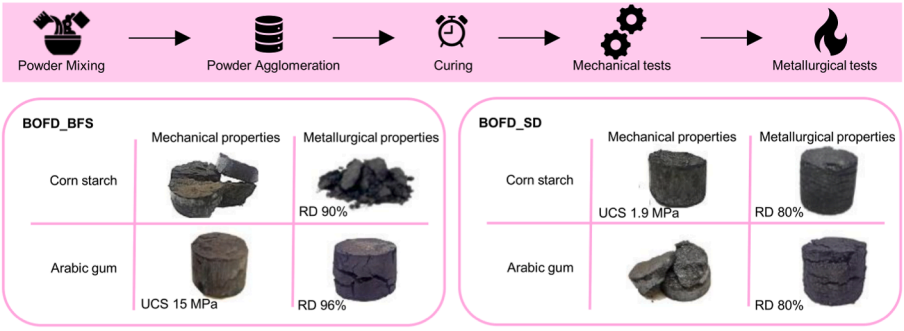

ARTICLE INFO

Keywords:
Agglomeration
Arabic gum
Starch
Integrated steel plant
By-product

ABSTRACT

The selection of a suitable binder is crucial to ensure efficient powder agglomeration and high mechanical stability of briquettes. In ironmaking and steelmaking, binders must have low silica, low ash, high environmental sustainability, and compatibility with furnace lining and slag. Gelatinized corn starch has shown good performance with several residues (e.g., jarosite, red mud, mill scale), but it has not provided consistent results when used with integrated steel-plant by-products. This study investigated the possibility of replacing corn starch with Arabic gum, analyzing briquettes produced from basic oxygen furnace dust combined with two reducing agents: blast furnace sludge (BFS) and secondary dust (SD). Arabic gum improved impact resistance index of BFS-containing agglomerates reaching IRI of 1000 (125 with starch), due to better particle arrangement and densification. The resulting lower porosity (34.3 % Vs 39.3 %) enhanced contact between carbon and iron oxides, raising the reduction degree to 90 % (86 % with starch). Moreover, the denser microstructure limited the swelling phenomenon observed in starch-bound briquettes during thermal treatment. In contrast, the use of SD as the reducing agent resulted in a coarser particle size, leading to a heterogeneous distribution during the mixing process with Arabic gum. This corresponded to a decrease in mechanical stability, with the briquettes surviving 5 drops compared to 10 with starch. Despite this drawback, the degree of reduction remained largely unaffected at 1200 °C.

* Corresponding author.
E-mail address: sara.scolari@polimi.it (S. Scolari).

https://doi.org/10.1016/j.partic.2026.01.008
Received 23 October 2025; Received in revised form 19 December 2025; Accepted 10 January 2026
Available online 16 January 2026

1. Introduction

Binders are substances that hold materials together, thereby enhancing the mechanical properties and stability of the final product (Trpčevská et al., 2015). In processes like agglomeration, binders are necessary to improve the compressive strength, hardness, and thermal stability of the agglomerated powders, making them easier to transport and handle than in their original form (Zhang et al., 2018). Initially, the binder must be liquid to ensure uniform distribution; then it forms an adhesive bond and hardens spontaneously (Trpčevská et al., 2015). An ideal binder should simultaneously provide a strong bond between the particles and be chemically compatible with the process it is involved in. Furthermore, its environmental friendliness and economic viability are two factors that must always be considered (Chen et al., 2025).

Several categories of binder have been used to agglomerate steelmaking-related products, such as slag, scale, sludge and dust (Alexander et al., 2023). Cement is one of the most common binders for aggregating iron ores, optimising the porosity of agglomerates and enhancing their density and compression strength. However, it suffers from low-temperature degradation and high slag formation (Alsaqoor et al., 2022). Another suitable option for bonding ore pellets is the use of bentonite, which is even better than cement due to its resistance at high temperatures (cement decomposes at over 400 °C (Liu & Chen, 2022)), while bentonite at 900 °C (Önal & Sarıkaya, 2007) and not burning away due to induration (Alsaqoor et al., 2022). However, the high percentage of silica in bentonite (45–65 wt% (Alsaqoor et al., 2022) raises the costs due to high overall energy consumption. Indeed, the lime-silica-based binder requires high energy to melt, increases the slag volume in the steelmaking processes, gives acidity and negatively affects the slag quality, making its employment not suitable in electric arc furnaces (EAFs) (Abdelrahim et al., 2022; Echterhof, Willms, Preiβ, et al., 2019) hence limiting its application in ironmaking processes (blast furnace and direct reduced iron (DRI)) only.

Consequently, organic binders are often preferred over inorganic ones because they contain less ash and silica, are more environmentally friendly, and enhance briquette porosity and reducibility (Alsaqoor et al., 2022; Zhang et al., 2018). Among them, a common example is starch, which is derived from plants such as corn, potatoes, and rice (Schirmer et al., 2015). In addition to its well-known use in food preparation, particularly in desserts, bread, pizza and soups, it is also frequently employed as a binder in metallurgical processes (Alsaqoor et al., 2022).

Several studies in the literature have used starch to agglomerate various by-products coming from the steelmaking (Dall'Osto, Mombelli, Scolari, & Mapelli, 2024; Dall'Osto, Mombelli, Scolari, & Mapelli, 2024; Drobíková et al., 2016; Lohmeier et al., 2020; Mombelli et al., 2021; Scolari, Mombelli, et al., 2025) because it generates capillary and molecular forces that improve adhesion and cohesion between particles, thereby enhancing the mechanical properties of the agglomerates (Mombelli et al., 2021). Additionally, the chemical composition of starch enabled it to be successfully used to agglomerate grinding sludge intended for EAF feeding (Echterhof, Willms, Preiss, et al., 2019).

Nevertheless, it is not applied directly to the raw powder mixture; instead, it requires a thermal treatment in water, during which starch first gelatinizes and then retrogrades. Gelatinization is essential for effective binding, as it makes the starch sufficiently sticky to hold the particles together (Han et al., 2014; Zhang et al., 2018), maintaining sufficient briquette integrity to be suitable for their management and transportation (Mombelli et al., 2021). The mechanism of gelatinization and following retrogradation was studied by (Lund & Lorenz, 1984; Sandhu & Singh, 2007), while Dall'Osto, Mombelli, Trombetta and Mapelli (2024) defined 30 % as the degree of retrogradation to get the best binding effect in briquettes produced with jarosite and blast furnace sludge.

However, subsequent studies (Dall'Osto, Mombelli, Trombetta, & Mapelli, 2024; Scolari, Mombelli, et al., 2025) have demonstrated that the properties of agglomerates are also influenced by the type of steelmaking residue used, even under identical binder conditions (e.g., category, amount, retrogradation degree). This could result in agglomerates that do not meet the desired mechanical specifications. In particular briquettes made of integrated cycle steel plant by-products (Scolari, Mombelli, et al., 2025) did not safety satisfy the industrial requirements getting Impact Resistance Index (IRI) close to the industrial benchmarked imposed (125 vs 97.7 (Adu-Poku et al., 2022)) and Ultimate Compressive Strength (UCS) lower than the minimum strength required in a basic oxygen furnace (1.90 vs 9.8 MPa (Barisetty et al., 2020)).

To address the above industrial applicability issues of the briquettes made in Basic Oxygen Furnace Dust and Blast Furnace Sludge (BOFD_BFS), as well as those made in BOFD and Secondary Dust (BOFD_SD), Arabic gum was selected as a sustainable alternative to corn starch for binding the two by-products of steel production. This approach preserves the beneficial properties of organic binders while maintaining synergy with the food industry.

Derived from Acacia trees, Arabic gum is widely employed in the food sector (e.g., wine and candy) to prevent sedimentation and keep liquid aromatic compounds in suspension. It is a high molecular weight polysaccharide covalently bonded with a protein fraction (Li et al., 2026), easily dissolvable in water and with a water absorption capacity (WAC) of about 45 % (Prasad et al., 2022). The polymeric chains allow to create a network which favor the binding effect (Li et al., 2014), due to the formation of an adsorbed liquid layer on particle surfaces, which smooths the surface and reduces interparticle distance through capillary action. This layer enhances adhesion forces, promotes collisions between wetted particles, and facilitates their agglomeration. Over time, liquid bonds can evolve into permanent solid bridges (Ghosal et al., 2010).

In literature, Arabic gum has mainly been employed as a binder in biomass briquettes. For instance, it has been mixed with rice husk to produce pellets for domestic heating in cooking stoves with low smoke emissions (Yahaya & Ibrahim, 2012), or used in Nigeria to briquette sawdust, mitigating the issues of pollution and poor thermal efficiency linked to its direct combustion (Okegbile et al., 2014). To the authors' knowledge, however, the only application of Arabic gum in metallurgical field is in the work of (Koohestani et al., 2025), where the organic binder was used to agglomerate magnetite iron ore. Although the slightly reduction in compressive strength (nearly 2.0 kN/pellet with bentonite and nearly 1.5 kN/pellet with Arabic gum), the 0.022 kN/pellet required for industrial application was largely satisfied using the gum (Ma et al., 2024; Sivrikaya & Arol, 2012). This study therefore encouraged the authors to follow this novel approach by exploring the Arabic gum potential for agglomerating metallurgical by-products. This choice is supported by (Omoniyi & Igbo, 2016), in which Arabic gum was shown to have superior binding performance, yielding rice husk briquettes with higher compression strength (4–5 kN m^{-2}) compared to starch (2 kN m^{-2}). Accordingly, the goal of this work is to evaluate the applicability and suitability of Arabic gum used as a binder in steelmaking by-products agglomeration, determining whether it could overcome the mechanical resistance limitations observed in BOFD_BFS briquettes bound with starch and preserving the stability of BOFD_SD by increasing its compressive resistance (Scolari, Mombelli, et al., 2025), without compromising their self-reduction capability.

2. Materials and methods

The materials used in this work were a hydrophilic sludge (BFS) coming from the dedusting of blast furnace off-gas sieved <63 μm, a hydrophobic dust (BOFD) coming from the abatement of basic oxygen furnace gas sieved <125 μm and a hydrophobic secondary dust (SD) separated after the cleaning of gases released during the desulphurization process sieved >125 μm. The raw materials were previously characterized by (Scolari, Mombelli, et al., 2025) including the evaluation of

water–powder interaction through sessile drop performed in accordance with BS EN ISO 19403 after compacting a few grams of powder into a disk following ASTM D7334-08 (2017), the assessment of particle size distribution via optical granulometry using a Malvern Morphology 4 granulometer (Malvern Panalytical Ltd., Malvern, UK), and the crystallographic and mineralogical characterization carried out through X-ray diffraction (XRD) analysis through Rigaku SmartLab SE diffractometer (Rigaku Corporation, Tokyo, Japan) in θ-θ configuration (Cu-Kα radiation: λ = 1.54 Å at 40 kV, 40 mA). The analysis was accomplished with a scan range of 5–90° 2θ through a 1D D/teX Ultra 250 detector featured by an XRF suppression filter; the powdered materials were scanned at 2° min^{-1} with a step size of 0.02° and rotated at 60 rpm. Their chemical composition, obtained by means of Wavelength Dispersion X-Ray Fluorescence (WD-XRF) through a Bruker S8 Tiger spectrometer (Bruker Corporation, Billerica, MA, USA), is reported in Table 1.

The powders were agglomerated in pairs, balancing the iron carrier and the reducing agents to tailor the amount of carbon to the equivalent Fe_2O_3 inside each mixture, guaranteeing the latter's complete reduction. The resulting ratios were 2.1:1 for BOFD_BFS and 1.2:1 for BOFD_SD. Two batches of the same mixture were prepared, with only the binder being changed: (1) corn starch (_CS) was dosed to reach 5 wt% of the total dry powders, it was than mixed with distilled water (a water/starch ratio of 6:1 by mass) and subsequently heated for 30 min at 100 °C to get retrogradation up to 30 % according to (Dall'Osto, Mombelli, Trombetta, & Mapelli, 2024); (2) Arabic gum (_AG) was mixed with distilled water (a water/gum ratio of 2:1 by mass) in a beaker covered with hollow lid to allow aeration for 24 h; then the beaker was closed for 7 days. It was then dosed to maintain the 5 wt% of the total dry powder.

Briquettes of 20 mm in diameter and 20 mm in height were produced using a modified uniaxial tensile test machine. A constant speed of 20 mm min^{-1} was applied until the pressure reached 40 MPa and then maintained for about 2 min. The mass variation of the briquettes was monitored during 15 days of curing at room temperature, and the apparent density of the green and cured briquettes was measured.

2.1. Mechanical characterization

The impact resistance of briquettes after curing has been evaluated through drop test, based on the ASTM D440−07 (2019). Each sample was manually released from a height of 1.63 m onto a steel container (~1 m^2) large enough to prevent material loss, using a 100 mm U-shaped steel semi-tube to ensure both vertical alignment and test repeatability. The test was repeated for each briquette and stopped either after 10 drops or earlier if a detached fragment exceeded 5 wt% of the briquette's initial mass. The size stability factor (*s*) of the briquettes was calculated with Eq. (1):

$$s = \sum_i \%\ wt_i \cdot NF_i \tag{1}$$

where wt_i is the weight of the *i-sm* fraction collected in each sieve with opening size of 6.7, 5.6, 4, 2, 1, 0.5 and 0.125 mm. NF_i is expressed as Eq. (2).

$$NF_i = \frac{(Opening_i + Opening_{i+1})/2}{(Opening_{max} + Opening_{max+1})/2} \tag{2}$$

The Impact Resistance Index (IRI) was calculated with Eq. (3) (Blesa et al., 2003). The average number of pieces was obtained counting the number of fragments that weighed 5 % or more than the initial mass of the briquette (Adu-Poku et al., 2022).

$$IRI = 100 \cdot \frac{Average\ number\ of\ drops}{Average\ number\ of\ pieces} \tag{3}$$

The Adjusted Impact Resistance Index (AIRI) (Eq. (4)) is a parameter that considers the powder detached during the drop test (Mombelli et al., 2021) and required the calculation of the Adjusting Factor (Eq. (5)), which was obtained from the Adjusting Mass Factor (Eq. (6)) calculated considering the mass retained in each sieve with an opening size smaller than 4 mm and the final mass collected at the end of the test

$$AIRI = IRI \cdot Adjusting\ Factor \tag{4}$$

$$Adjusting\ Factor = 1 - \frac{Adjusting\ Mass\ Factor}{Final\ mass} \tag{5}$$

$$Adjusting\ Mass\ Factor = \sum_i \frac{4}{S_i} \cdot M_i \tag{6}$$

where M_i is the mass retained by the *i-sm* sieve and S_i is the sieve opening passed. Lower AIRI corresponds to the detachment of finer particles, while AIRI much lower than IRI means a big amount of fine powder lost. If the Adjusting Factor is negative, it should be considered as zero.

If the briquette survived to 10 falls, it was then compressed according to BS ISO 4700:2015, to evaluate the ultimate compressive strength (UCS). The sample was pre-loaded between two flat plates at 30 N and pressed at a constant speed of 15 mm min^{-1} until the load falls by 50 % of the ultimate compressive strength (UCS) or when the gap between the plates was reduced by more than 50 % of the briquette diameter (10 mm).

2.2. Metallurgical characterization

Briquettes have been thermally treated at 700, 950 and 1200 °C inside a Nabertherm LBT 02/17 lift-bottom furnace (Nabertherm GmbH, Lilienthal, Germany) using an inert atmosphere (Ar) by imposing a heating ramp of 100 °C min^{-1} and the maintenance time of 15 min at the desired temperature. The reduction degree (Eq. (7) (Li et al., 2023)) was inspired by BS ISO 11258:2015.

$$RD = \frac{m_{wet} - m_{HT}}{m_c + m_O + m_{binder} + m_{volatile}} \times 100 \tag{7}$$

where m_{wet} is the mass of the green briquette, m_{HT} is the mass of the reduced briquette. The theoretical maximum loss of mass achieved by the mixture completely reduced at 1500 °C has been evaluated starting from the initial chemical composition of the briquettes and considering the masses of volatile compounds such as Zn, Cl and alkalis as $m_{volatile}$, the oxygen (m_o) released during the reduction, carbon mass (m_c) consumed and the binder which completely volatilizes during the heating.

Swelling index was calculated according to BS ISO 4698:2022. Eq. (8) considers the apparent volume, neglecting the internal porosities of agglomerates.

$$Swelling = \frac{\Delta V}{V_i} \times 100 \tag{8}$$

where ΔV is the difference between the volume of the briquette after the

Table 1
Chemical composition of Blast Furnace Sludge (BFS), Basic Oxygen Furnace Dust (BOFD), and Secondary Dust (SD) expressed in wt.% ("-" means not detected).

Sample	Alkali	Al_2O_3	CaO	Cl	Cr_2O_3	Ctot.	Fe_2O_3	MgO	MnO	NiO	P_2O_5	S	SiO_2	SnO_2	ZnO
BFS	1.22	2.01	3.50	–	0.66	41.81	38.96	0.77	0.14	–	–	0.87	5.94	0.14	1.93
BOFD	0.50	0.24	6.69	0.25	–	3.71	77.54	2.62	1.03	0.10	0.18	0.21	2.17	–	2.16
SD	0.12	0.06	10.67	–	–	31.13	46.69	1.58	3.57	–	0.08	0.22	1.37	–	1.61

thermal treatment and its initial volume V_i. V_i was calculated assuming the briquette as a perfect cylinder, whereas the volume after the thermal treatments was evaluated through photogrammetry using Evixscan 3D (Evatronix SA, Wiktora Przybyły, Bielsko-Biała, Polonia) which reproduced, as mesh, the body of the briquette. Structured light scanning involves projecting patterns of a present structure onto a scanned object. Two cameras then take a series of images in the same area. Based on the deformation of the patterns, an algorithm generates a point cloud that is automatically triangulated into a triangle mesh describing the scanned shape. MeshLab has been subsequently used to do the surface reconstruction, creating watertight surfaces from oriented point sets and to calculate the volume.

The morphology and the semi-quantitative chemical analysis of pre- and post-reduced briquettes were analyzed through a Zeiss Sigma 300 Field Emission Gun Scanning Electron Microscope (FEG-SEM) equipped with an Oxford Xmax Ultim 65 Energy-Dispersive X-Ray Spectroscopy (EDS) probe (Oxford INCA, Oxford Instruments, High Wycombe, UK). The porosity of the cured briquettes was calculated according to (Ezeakacha et al., 2018; Rabbani & Salehi, 2017). The darker spaces inside the SEM images detected using Otsu multi-level thresholding over gray-scale are considered as porous and they are measured using the algorithm Watershed. The post-heat treatment briquettes also underwent crystallographic analysis and minerals identification by means X-Ray diffraction (XRD).

3. Results and discussion

3.1. Mechanical characterization

The appearance of the mixtures BOFD_BFS and BOFD_SD agglomerated with both starch (_CS) and Arabic gum (_AG) in form of self-reducing briquettes is shown in Fig. 1.

On the one hand, the coloring of the briquettes was dependent from the reducing agent involved. BFS produced a blackish appearance, SD favored brightness and the formation of red rust bubbles due to its hydrophobicity (Scolari, Mombelli, et al., 2025). On the other, the surface finishing was affected by the organic binders used. Corn starch caused a higher development of macrocracks after the agglomeration of fine BFS than Arabic gum. Indeed, BOFD_BFS_CS (Fig. 1a) appeared less compact than BOFD_BFS_AG (Fig. 1b), which had a more homogeneous and closely packed lateral surface. Conversely, the Arabic gum reduced the mechanical stability of the agglomerates when coarse SD were present, as evidenced by the greater number of cracks on the surface of BOFD_SD_AG (Fig. 1d) compared to BOFD_SD_CS (Fig. 1c).

The mass variation monitored during the curing time is shown in Fig. 2.

The maximum mass loss obtained for the agglomerates prepared with Arabic gum was about 5 %, regardless of the type of mixture. In comparison, starch led to a slightly higher mass reduction for BOFD_SD_CS (5.7 %) and up to 9 % for BOFD_BFS_CS, which can be attributed the higher free water of the starch than Arabic gum (Okegbile et al., 2014). To better understand how the binders affected the mass loss of the briquettes, their mass loss rate was examined and shown in Fig. 2(b). Although the use of different binders, BOFD_SD_AG and BOFD_SD_CS showed very similar behaviour, both stabilizing after the first week of curing. The mixture BOFD_SD demonstrated that the type of binder used did not affect the mass loss rate of a mixture which contained only hydrophobic particles, but it depended solely on the interaction between the water and the powder. As already demonstrated by (Scolari, Mombelli, et al., 2025), the briquettes immediately lost the free available water due to the nature of the powder itself. Different considerations were done in presence of hydrophilic particles as BFS, where the type of binder plays a key role. BOFD_BFS_AG indeed followed a comparable mass loss rate with the above mixture, while BOFD_BFS_CS showed a continuous mass loss over the entire curing period. These different behaviours were attributed to the physical nature of the binders and their binding mechanism. The retrogradation of starch released water which is progressively adsorbed and exuded from the powders causing a delay in the water release kinetics (Wang et al., 2015), as happened in BOFD_BFS_CS. This mechanism accounts for both the higher mass loss and the absence of stabilization (Scolari, Mombelli, et al., 2025). On the contrary the use of a liquid binder as Arabic gum allowed a direct contact between dust and moisture with an immediate release of water. The consequence was that, despite the presence of hydrophilic BFS, the powders behaved as if they were completely hydrophobic, hence releasing all the free water during the first week of curing. This explained why the stabilization rates of BOFD_SD_AG, BOFD_SD_CS and BOFD_BFS_AG were similar, while that of BOFD_BFS_CS was completely different.

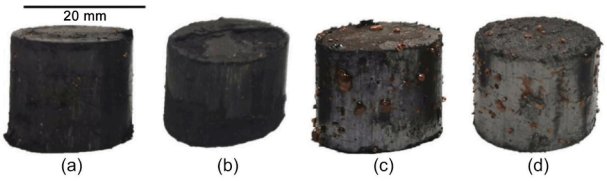

Fig. 1. Appearance of green briquettes (a) BOFD_BFS_CS; (b) BOFD_BFS_AG; (c) BOFD_SD_CS; (d) BOFD_SD_AG.

The apparent density of green and cured briquettes and their mechanical properties are reported in Table 2.

The effect of the binder in the apparent density of the agglomerates depended on the particle size distribution (PSD) of the reducing agents. In the presence of fine BFS, the Arabic gum considerably densified the agglomerates, while changing the binder in briquettes with coarse SD had a negligible effect on density. BOFD_BFS_AG indeed showed an apparent density 10 % higher than BOFD_BFS_CS. This density improvement could be attributed to the higher amount of water immediately available in the gum compared to the starch, which promoted stronger interactions with the hydrophilic BFS particles. As already observed in the previous work of (Scolari, Mombelli, et al., 2025), a higher water content in BOFD_BFS mixture favored briquette densification, likely due to the tendency of hydrophilic particles as BFS to bind with water. Conversely, no significant variation in density was observed between BOFD_SD_AG and BOFD_SD_CS (1.17 %), indicating that the free water in the Arabic gum did not improve the packing of the particles, which was already optimized by a homogeneous particle size distribution. The above assumption was confirmed by Tukey test which indicated the significative effect of the binder on the densification of BOFD_BFS and the no-significative effect of the same parameter on BOFD_SD (see Supplementary Table S1).

The same relationship between the PSD and the binder used, which affects the density of the agglomerates, was found in the literature. Indeed, briquettes made of grinded *Azadirachta indica* charcoal agglomerated with Arabic gum were 1.28 times denser than those made with starch (Sotannde et al., 2012), while (Ezechiel et al., 2022) defined a similar density of briquettes made of rice husks sieved with opening size of 0.5 mm independently from the binder used. These findings confirmed that it is impossible to establish a generic rule for how binders affect the agglomerate's density. However, they emphasized that the combined effect of physical properties of powders and the type of binder used should also be considered when determining briquette density.

The importance to consider the effect of the binder in addition to the physical properties of the powders (e.g., PSD and water-powder interaction) was also evident evaluating the mechanical properties of the briquettes (Table 2). For instance, not only did the Arabic gum favor the correct arrangement of BOFD_BFS_AG resulting in densification, but the elevated quantity of free water in the binder also gave benefits in the initial bonding of fine particles resulting in higher resistance (Patil et al., 2009; Sen et al., 2016). BOFD_BFS_CS broke after an average of 4.67 ± 2.89 drops, whereas BOFD_BFS_AG survived up to 10.00 ± 0.00

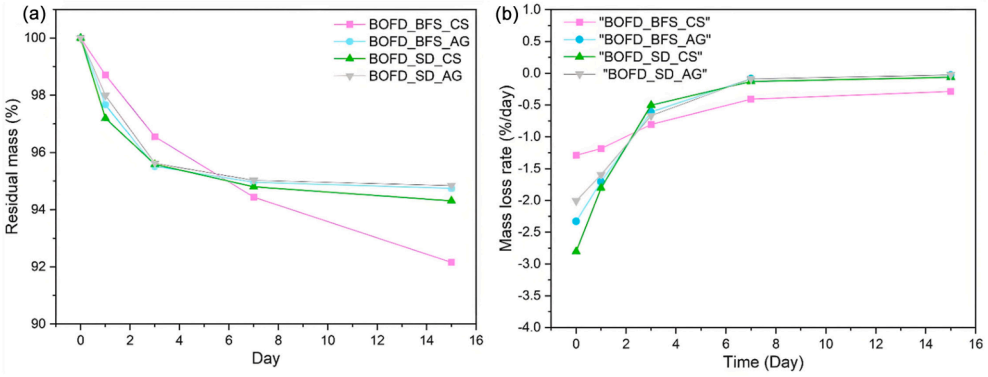

Fig. 2. (a) Mass reduction of briquettes during curing time; (b) Mass loss rate of briquettes during curing time.

Table 2
Apparent density of green and cured briquettes and their mechanical properties (IRI, AIRI and size stability).

Sample	Green density (g cm^{-3})	Cured density (g cm^{-3})	IRI	AIRI	Size stability (%)
BOFD_BFS_CS	2.44 ± 0.03	2.25 ± 0.04	125.00 ± 66.14	23.68 ± 23.56	86.30 ± 4.02
BOFD_BFS_AG	2.64 ± 0.03	2.51 ± 0.04	1000.00 ± 0.00	902.02 ± 12.84	98.83 ± 0.08
BOFD_SD_CS	2.49 ± 0.02	2.35 ± 0.02	1000.00 ± 0.00	649.47 ± 102.83	93.35 ± 0.81
BOFD_SD_AG	2.41 ± 0.02	2.31 ± 0.03	188.89 ± 101.8	93.44 ± 26.84	94.17 ± 5.97

drops; the IRI-AIRI difference for BOFD_BFS_CS was 81.06 %, whereas Arabic gum reduced it to 9.80 %, indicating a lower amount of fine dispersion and finally, the liquid binder improved the size stability by 14.5 %. The higher amount of water in Arabic gum increased the mechanical resistance of briquettes made of hydrophilic sludge probably because the BFS was completely saturated with absorbed water. The saturation enhanced the cohesive forces between the particles (Olugbade et al., 2019) instead of generating a repulsive behavior typical of hydrophobic-hydrophilic interaction (Kopel & Giovambattista, 2019), as already happened in the optimization process of the previous work (Scolari, Mombelli, et al., 2025) where improvements of BOFD_BFS_CS properties were obtained only after doubling the water during starch gelatinization. A comparable mechanical improvement was observed when the water content was doubled in the red mud–BFS agglomeration process. In this system, the amount of water clearly emerges as a key parameter to be optimized, since the free water available during powder mixing promotes an efficient rearrangement and coalescence of the particles (Scolari, Dall'Osto et al., 2025). The same effect was achieved when using Arabic gum, which, being a water-based liquid solution, intrinsically provides the necessary moisture to favor particle interaction, without the need to wait for starch retrogradation. Different evidences were instead defined changing the binder in presence of the coarse SD. Despite no significant variation in density with respect to BOFD_SD_CS, a worsening in resistance was shown by BOFD_SD_AG which broke after 5.00 ± 1.00 drops (BOFD_SD_CS survived to 10.00 ± 0.00 drops). However, it was a predictable result due to more cracked surface of the BOFD_SD_AG and the knowledge of the worsening of the linkage between coarse particles by the action of Arabic gum (Patil et al., 2009). The excess of water negatively interfered with the cavitation behavior typical of hydrophobic-hydrophobic interaction (Kopel & Giovambattista, 2019) leading to a worsening in the mechanical properties of BOFD_SD_AG compared to BOFD_SD_CS. The significant effect on the mechanical properties of the briquettes changing the binder was also confirmed by the Tukey test reported in Tables S2, S3 and S4 in supplementary materials.

Despite the failure of BOFD_BFS_CS and BOFD_SD_AG after nearly 5 drops, all the agglomerates had IRI higher than the Italian standard defined for briquettes (97.7) (Adu-Poku et al., 2022) and survived to a number of drops greater than 4, which is considered the benchmark value for the iron ore agglomerates (Seetharaman, 2013). Although the mechanical requirements for the BOFD_BFS_CS briquettes were met, the authors consider the agglomerates to be risky for correct handling, with an IRI only 30 % higher than the industrial benchmark. Therefore, improving the impact resistance using Arabic gum is strongly recommended to ensure that the BOFD_BFS mixture can be used safely and hence significantly reducing the fines dispersion. Conversely, the addition of Arabic gum reduced the impact resistance of the BOFD_SD mixtures, decreasing the IRI by 81 %. This makes corn starch a more suitable alternative for the latter mixture.

Being survived to 10 drops, BOFD_BFS_AG and BOFD_SD_CS was then compressed leading to UCS of 15.86 ± 1.22 MPa and 1.90 ± 1.30 MPa, respectively. Also, BOFD_BFS_AG formed less than 1 % of dispersed fine below 500 μm during the compression, evidence of a good and successful agglomeration process. On the contrary, BOFD_SD_CS presented many limits in transport and storage since compressive strength was close to 1 MPa (Borowski et al., 2017). Its low compression resistance could be related to its low density (Philippe et al., 2018).

If the chemical composition of the raw materials were compatible with the furnaces, BOFD_BFS_AG would be the only mixture suitable for industrial applications, considering that a cold compressive strength of 300 N/pellet is required for special shaft furnaces, such as those used in the Tecnored process (Mantovani & Takano, 2000), and the CCS for using briquettes inside a converter is 100 kg cm^{-2} (9.8 MPa) (Barisetty et al., 2020).

The good compression resistance of BOFD_BFS_AG was the result of the appropriate particles agglomeration and densification favored by the hydrophilic nature of BFS. To better understand the role of the binder in the agglomeration of the steelmaking by-products and the resulting mechanical resistance of briquettes previously discussed, SEM analysis was performed to investigate how the raw materials were arranged and packed. The particles arrangement given by starch in the BOFD_BFS_CS sample (Fig. 3a) revealed a porosity of 39.3 %, leading to poor agglomeration and unstable packing. In contrast, Arabic gum, used in the BOFD_BFS_AG sample (Fig. 3b), produced a flatter and more continuous matrix characterized by a porosity of 34.3 %, namely approximately 13 % less than promoted by starch.

Unlike starch, which did not exhibit strong adhesive properties, Arabic gum has highly sticky and glue-like consistency which improved particle cohesion and promoted stronger agglomeration. As a result, the overall particle arrangement became more uniform and compact,

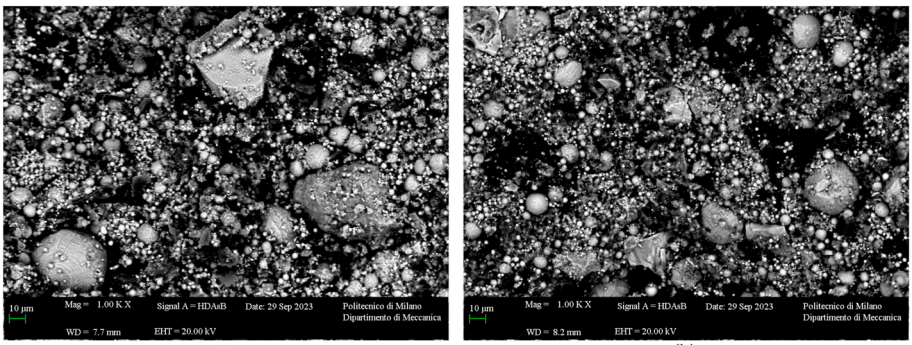

(a) (b)

Fig. 3. BSE-SEM image of (a) BOFD_BFS_CS; (b) BOFD_BFS_AG.

increasing density and, in turn, enhancing the briquette mechanical properties (Kotta et al., 2019). The possibility to enhance cohesiveness between particles with Arabic gum was even more evident in BOFD_SD mixture. BOFD_SD_CS (Fig. 4a) appeared more porous (porosity of 14.3 %) and less compact, with many voids near the bigger particles of SD, while BOFD_SD_AG (Fig. 4b) shows a better cohesiveness between the particles with a consequent reduction of porosities (dropped to 9.8 %).

Ferreira et al. (2022) described the same evident loss of porosity found in BOFD_SD_AG and attributed this phenomenon to the Arabic gum capacity of filling the free spaces surrounding the particles. Therefore, additional BSE-SEM and SEM-EDS were performed to investigate the inner structure of the briquettes and understand why the mechanical properties of BOFD_SD_AG were reduced despite the particles being more compactly distributed.

Despite a reduction in porosity of 31 % using the liquid Arabic gum binder, decreasing the magnification it was evident that the particles arrangement in BOFD_SD_AG was extremely heterogeneous compared to BOFD_SD_AG. Fig. 5(a) shows a good dispersion of finer and coarser particles, while Fig. 5(b) revealed an inhomogeneous particles distribution inside the briquette with the formation of clusters of fine particles (A in figure, which is shown at higher magnification in Fig. 4b) around the big particles of carbon (B in figure). This strong clustering due to the specific PSD of both selected raw materials affected the packing of the particles, leading to heterogeneity of the internal structure of the briquettes. This was the main cause for the reduction of the impact resistance of the mixture.

The clustering effect was achieved not only through the penetration of liquid Arabic gum among the carbon particles and the dragging of finer oxides, but also through the clustering of the Arabic gum itself amongst the fines. Arabic gum is polysaccharides in the form of salt of calcium, magnesium and potassium, where the first element is one of the principal constituents (Jarrar et al., 2021; Prasad et al., 2022). It was hence reasonable to consider the yellowish zone rich in calcium, identified as C in Fig. 6, as the binder itself. In addition, these zones were characterized by particles with a compact and spheroidal shape with a

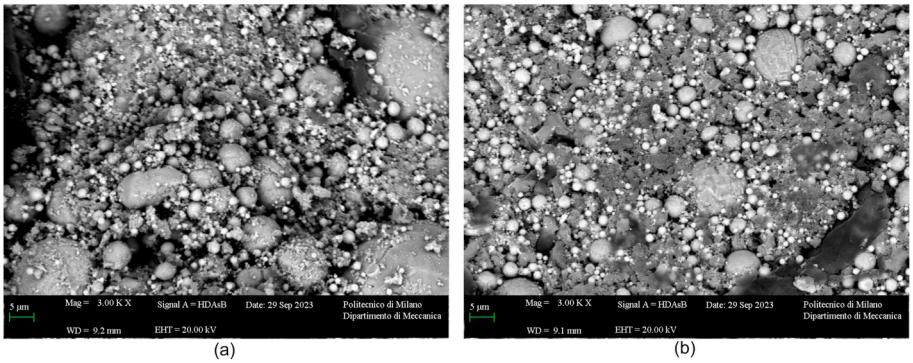

(a) (b)

Fig. 4. BSE-SEM image of cured (a) BOFD_SD_CS; (b) BOFD_SD_AG.

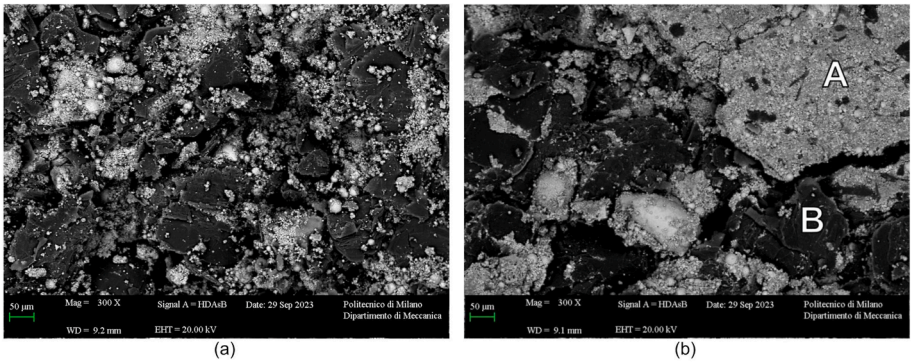

(a) (b)

Fig. 5. BSE_SEM of cured BOFD_SD_AG at low magnification.

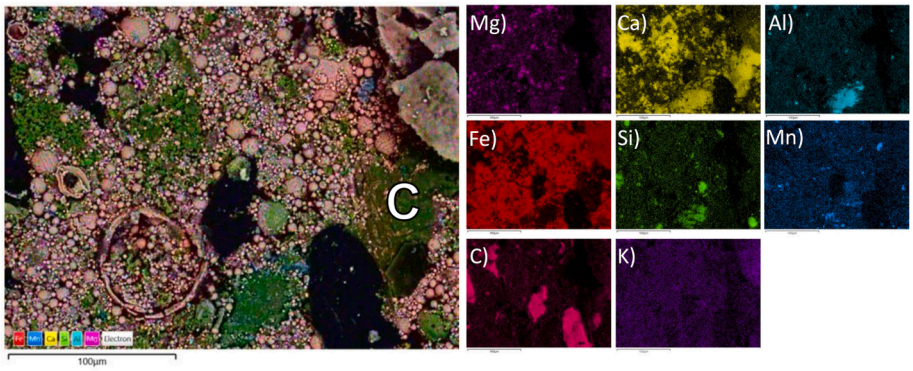

Fig. 6. EDS-SEM of cured BOFD_SD_AG.

diameter of less than 10 nm. This morphology was attributed to the polymeric phase of the gum and was found to be very similar to that obtained from cryo-TEM micrographs of an aqueous Arabic gum solution (Dror et al., 2006).

Despite Arabic gum being used in BOFD_BFS_AG as well, it did not exhibit this clustered structure. This is because the effect of the binder on powder agglomeration depends on the PSD of the dust used. Arabic gum was most likely able to maintain a homogeneous distribution during the agglomeration of fine particles, increasing the mechanical resistance of BOFD_BFS. On the contrary, it dripped around the large fragments of SD, favoring the clustering of the finer fraction and causing a heterogeneous structure, which worsened the mechanical properties of BOFD_SD.

3.2. Metallurgical characterization

The degree of reduction of the briquettes thermally treated at 700, 950 and 1200 °C is shown in Fig. 7. In addition to the above mechanical characterization, the self-reduction capability of the briquettes depended on the combined effect of the PSD of the reducing agent used in the mixture and the binder. BOFD_BFS_AG showed an increase in RD of 4.36 % compared to BOFD_BFS_CS. As the self-reduction process is based on a carbothermic reaction, the more uniform and compact particle distribution with reduction in porosity inside BOFD_BFS_AG (Fig. 3) enhanced the contact area between the carbon and the iron oxides. Consequently, the reduction efficiency increased (Kowitwarangkul et al., 2014). In addition, the chemical structure of the binder used (Prasad et al., 2022) suggested that Arabic gum ($(C_5H_8O_4)n(C_{14}H_{23}O_{10})m$) may contain a greater amount of carbon than starch ($(C_6H_{10}O_5)n$), thereby improving the reduction performance of the mixture.

Although the chemical composition of the Arabic gum should increase the self-reduction capability of the briquettes, the reduction degree of BOFD_SD_CS and BOFD_SD_AG did not show significant variation (0.5 %) and the absolute value was still lower than that of BOFD_BFS. The high carbon content of Arabic gum was therefore unable to overcome the limitation of excessive coarseness of the reducing agent in reducing iron oxides to metallic iron. The coarse dimension of the SD limited the carbothermal reduction because large carbon fragments had a low surface area for contact with iron oxides (Scolari, Mombelli, et al., 2025). Consequently, self-reduction only occurred at the interface, resulting in poorer metallurgical performance (Kowitwarangkul et al., 2014). Nevertheless, the heterogeneous particle distribution and clustering of the iron oxides-containing fraction induced by Arabic gum did not negatively affect the metallurgical behavior of the BOFD-SD mixture.

XRD analysis (Fig. 8) on the reduced briquettes at 1200 °C was performed to ensure that the choice of the binder did not affect

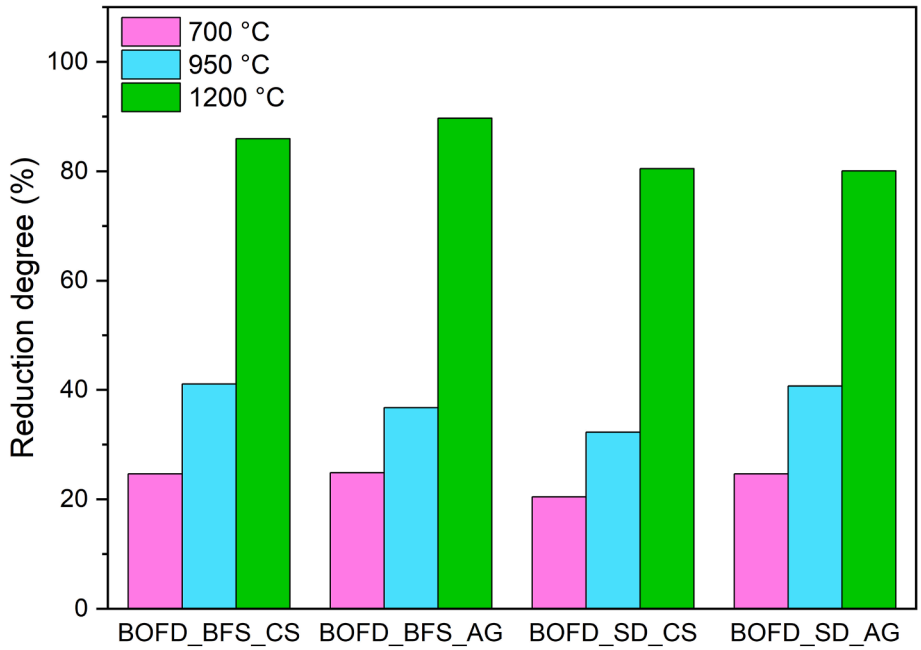

Fig. 7. Degree of reduction expressed in % of the briquettes reduced at 700, 950 and 1200 °C.

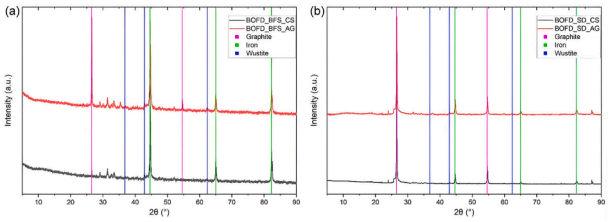

Fig. 8. XRD patterns of reduced (a) BOFD_BFS_CS and BOFD_BFS_AG; (b) BOFD_SD_CS and BOFD_SD_CS. The undefined peaks are the peaks characteristic of slag.

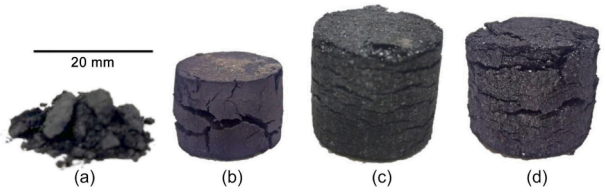

Fig. 9. Appearance of briquettes reduced at 1200 °C (a) BOFD_BFS_CS; (b) BOFD_BFS_AG; (c) BOFD_SD_CS; (d) BOFD_SD_AG.

qualitatively the chemical and metallurgical reactions during the reduction process. The satisfying metallurgical performances were confirmed by the presence of the metallic iron peak and absence of hematite (Fe_2O_3) and magnetite (Fe_3O_4) peaks. However, both the mixtures had some unreduced iron oxide in form of wustite (FeO) and a slag phase identified mainly as gehlenite ($Ca_2Al[AlSiO_7]$). Despite the peaks having different intensities, the XRD patterns of the reduced briquettes made from the same mixture, but agglomerated using the two binders, were perfectly superimposable on each other. This ensured that starch and Arabic gum could be used indiscriminately without affecting the self-reducing reactions from a reduction point of view. However, the reduction of graphite peaks and the intensification of metallic iron peaks in BOFD_BFS_AG confirmed its higher degree of reduction than in BOFD_BFS_CS, while the same peaks intensity observed in the BOFD_SD patterns confirmed the similarity of the RD obtained between the two mixtures.

Looking at the appearance of briquettes reduced at 1200 °C (Fig. 9), Arabic gum was able to maintain the self-standing capacity of both mixtures, thereby overcoming the instability found in BOFD_BFS_CS. Despite the evident cracks all along its surface, BOFD_BFS_AG showed the compact and robust appearance characteristic of smelting, which is caused by the solidification of the metallic network and the melting of the slag, thereby filling the voids left by carbon consumption (Huang et al., 2019). The glue power of Arabic gum was hence able to overcome the disruptive forces inside BOFD_BFS. Therefore, the low porosity resulting from the densification and homogeneous particle distribution provided by the Arabic gum in the fine particle aggregates was the key to maintain the agglomerate's mechanical stability also at high temperature.

Conversely, although the binder preserved the agglomerated shape of BOFD_SD mixture, the adhesive properties of the Arabic gum could not withstand the expansion of the briquette made of coarse SD particles. BOFD_SD_CS and BOFD_SD_AG indeed appeared swollen at 1200 °C and more fragile than at room temperature. Many cracks developed in different directions. They created a no uniform and uncompact surface, but rather they highlighted the presence of an unstable group of particles that were not strongly bound together. Singh and Bjorkman (2004b) also described the same variation in appearance of the agglomerates according to the PSD of the powders: a more compact appearance with d_{50} lower than 74 μm, and the formation of many cracks in any direction with coarser particles.

Arabic gum gave self-standing stability to briquettes with BFS reduced at any temperature solving the problems found with

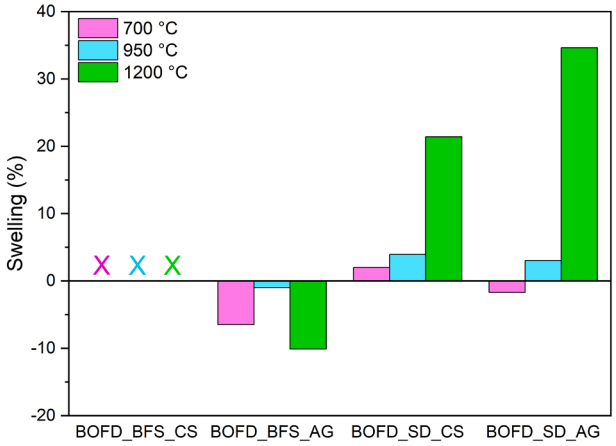

Fig. 10. Swelling behavior of briquettes reduced at 700, 950 and 1200 °C. ("X" means that the briquette was removed in pieces from the crucible after the corresponding thermal treatment).

BOFD_BFS_CS (Fig. 10). BOFD_BFS_AG presented the typical volume variation described in literature. The volume increased during heating from 700 to 950 °C, followed by shrinkage at 1200 °C (−6.48, −0.97 and −10.10 %, respectively) (Singh & Bjorkman, 2004b).

On the contrary, Arabic gum not limited the expansion of briquettes containing SD, which was further increased. The catastrophic swelling of BOFD_SD_AG at 1200 °C compared to BOFD_SD_CS indeed increased by 61.67 %. The swelling of BOFD_SD_CS was caused by (1) the delayed kinetic caused by coarse reducing agent; (2); the popping up of big particles (Singh & Bjorkman, 2004a) and (3) the low amount of silica that favored the separation of particles in the briquettes (Wang & Sohn, 2011). Explicitly, the coarse SD were responsible for an intrinsic kinetic delay of iron oxides reduction. Consequently, the briquettes did not exhibit the typical shrinkage behavior expected at 1200 °C; instead, they behaved as if the process were occurring at around 950 °C, a temperature typically associated with swelling phenomena (Scolari, Mombelli, et al., 2025). The swelling was further increased by the pressure generated by the large carbon fragments which pushed against each other. The pushing pressure was favored by the difference in the particle density (2.26 g cm^{-3} for carbon and 7.87 g cm^{-3} for iron oxides) (Singh & Bjorkman, 2004a; Strezov et al., 2005). In addition to these phenomena, the more pronounced swelling of BOFD_SD_AG was given by the heterogeneous particles arrangement identified in Fig. 5(b), which caused an additional volume expansion summed to the natural expansion given by the intrinsic characteristics of this mixture, resulting into a catastrophic swelling of nearly 35 %. The physical separation between coarse and fine particles due to the BOFD_SD_AG inhomogeneous structure, indeed allowed the bigger one to expand in easier way because of the clustering of the finer oxide around the big fragments of carbon. This left more space to the latter to freely push outside.

To better understand the effect of the Arabic gum on the particles' arrangement after the briquette reduction at 1200 °C, a BSE-SEM analysis was performed. The results of the BOFD_BFS mixture agglomerated with the two binders are shown in Fig. 11. Common evidence to both mixtures is that the particles lost their small and circular shape during the reduction at 1200 °C, leading to a smoother and elongated shape well clustered (Singh & Bjorkman, 2004b). However, as already identified at room temperature (Fig. 3), BOFD_BFS_CS (Fig. 11a) was characterized by a less uniform, inhomogeneous and more porous particles arrangement than BOFD_BFS_AG (Fig. 11b) (porosity of 46.1 % and 30.5 %, respectively). This was a consequence of the initial better packing given by the Arabic gum with favored the cohesion of the particles even after the reduction. Despite both briquettes showed the classic porosity caused by carbon consumption during reduction, the slag, melted in BOFD_BFS_AG, surrounded the iron and filled the

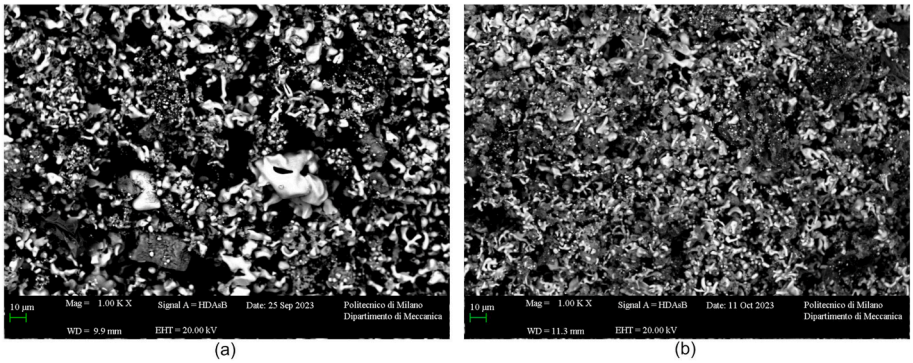

Fig. 11. BSE-SEM of briquettes reduced at 1200 °C (a) BOFD_BFS_CS; (b) BOFD_BFS_AG.

residual cavities (Fig. 11b). This resulted in the compact, resistant and shrunk appearance observed after the removal of the briquette from the crucible (Mombelli et al., 2016). This phenomenon was evident only using Arabic gum because the calcium concentration inside the binder increased the basicity of the mixture resulting in the decrease of the melting point of the slag (Wu et al., 2012).

In addition, in BOFD_BFS_AG both smelted iron and some short and thick iron whiskers coexist. The iron whiskers formation generally leads to swelling, but BOFD_BFS_AG shrank. This contradictorily situation was also noticed by (Wang & Sohn, 2011) which explained that shrinkage happens when the whiskers become larger in diameter and shorter in length. At 1200 °C, they indeed tend to coalesce together, passing from 3-5 µm to 5–12 µm of thickness (Fuwa & Ba N-Ya, 1969). Dimension which agrees with the thickness of the iron particles in Fig. 11b being favored by the CaO contained in the Arabic gum (Zhao et al., 2013). Indeed, in presence of enough availability of CaO, generally higher than 4 wt%, whiskers may thicken otherwise they may only nucleate remaining short (about 3–5 µm) and thin (diameter of 0.8 µm) (Zhao et al., 2013). Hence, although whiskers are there, their negative effect is counteracted by both their coalesced morphology and slag formation, overall resulting in a volume shrinkage. Although a similar morphology can be observed for BOFD_SD_AG (Fig. 12b), this situation remains confined only in the region where fine iron oxides particles reduced to metal, without any beneficial effect in contrasting the swelling due to the above listed reasons.

On the contrary, the briquettes manufactured with corn starch (BOFD_BFS_CS - Fig. 11a and BOFD_SD_CS - Fig. 12a) do not exhibit iron whisker since the corn starch did not supply the additional calcium to the mixture to stimulate their nucleation and growth.

The Arabic gum concentrated around the spherical oxide particles identified at room temperature (Fig. 6) in BOFD_SD_AG had disappeared during the thermal treatments leaving some voids. Thermogravimetric analysis of Arabic gum indeed defined around 300 °C the disintegration temperature of the gum due to the polysaccharides' breakage (Mothe Â & Rao, 2000). The disappearance of the organic binder was also confirmed by (Koohestani et al., 2025) showing the complete removal of Arabic gum after the thermal treatment of iron ore pellets. Prolongated heating at higher temperatures causes the protein decomposition and subsequently the sugar loss. This induces the decrease of the Arabic gum viscosity decreasing its binding effect (Chikamai et al., 1996). The disappearance of the glue around the particles was an additional reason for the BOFD_SD_AG appearing as a set of small particles close together without any strong binding, making it appears more fragile than the BOFD_SD_CS. However, while the actual thermal behavior of Arabic gum mixed with integrated cycle steel plant by-products in an argon atmosphere is unknown to the authors, it is reasonable to assume that some of the binder remained in the briquette. For instance, considering the BOFD_BFS mixture, the disruptive forces found in BOFD_BFS_CS was overcome by the residual Arabic gum which kept the particles of BOFD_BFS_AG together.

3.3. Industrial feasibility of using a Recycled Arabic gum

One of the main problems associated with the using of Arabic gum is its high cost, due to its limited availability in local market (Ezechiel et al., 2022). Sudan is the primary producer (https://Bayrony.Com/Product-Enquiry/Products/Gum-Arabic/) and exports the natural gum world-wide at a price of 7.62 $ kg^{-1} (https://Www.Tridge.Com/Intelligences/Arabic-Gum/Price;LastAccess01/09/2025). In contrast, the price of corn starch is around 0.387 $ kg^{-1} (https://Procurementtactics.Com/Corn-Starch-Prices/?V=1a13105b7e4e;LastAccess01/09/2025). Although more water is required to prepare the gelatinized starch than the Arabic gum solution (6:1 and 2:1 water-to-solid ratio, respectively), the cost of water is negligible in the final calculation, being equal to 0.002 $ kg^{-1} (https://Www.Waternewseurope.Com/Water-Prices-Compared-in-36-Eu-Cities/;LastAccess01/09/2025). This would result in a cost of 0.0004 $ to prepare the gelatinized starch necessary to bind 1 kg of powder, compared to 0.017 $ for the Arabic gum. Despite that, the cost of

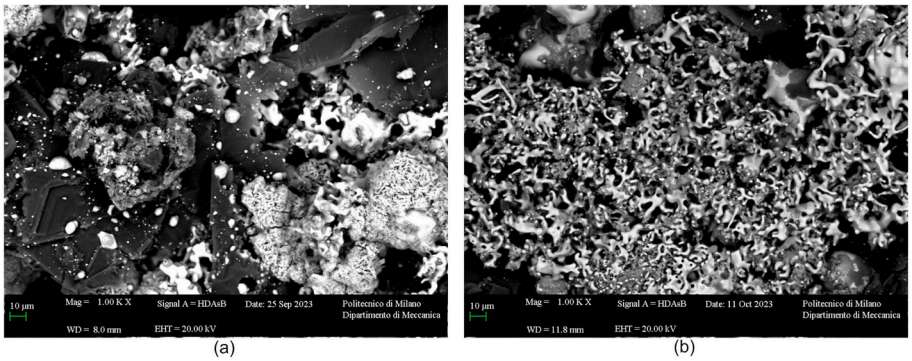

Fig. 12. BSE-SEM of briquettes reduced at 1200 °C (a) BOFD_SD_CS; (b) BOFD_SD_AG.

starch could increase drastically if electricity were used to heat the distilled water and starch to 105 °C. Considering the cost of electricity at around 0.2 $ kWh^{-1} (https://Ec.Europa.Eu/Eurostat/Statistics-Explained/Index.Php?Title=Electricity_price_statistics;LastAccess01/09/2025), an additional 4 $ should be added to the price of starch. However, the cost of heating the starch at 105 °C could easily avoided by recovering heat within one of the multiple sources of hot waste gas largely available in industry, especially in a metallurgical plant.

Being Arabic gum an expensive material, the improvements in the mechanical properties of BOFD_BFS mixture suggest the need to find a suitable and cheaper alternative to the natural powder extracted from acacia trees. One possibility is to recycle an Arabic gum solution coming from the food industry to maintain the synergy with steelmaking through a circular process. Arabic gum is commonly used in wine production to protect colloidal substances, improve foam stability, and prevent coloring matter from precipitating in red wine (Apolinar-Valiente et al., 2020; Nigen et al., 2019; Sanchez et al., 2018). The process involves the production of a waste based on Arabic gum which could be recycled as binder in the agglomeration of steelmaking by-products.

In order to evaluate the effects on the mechanical and metallurgical properties of briquettes after the substitution of the natural Arabic gum with the recycled solution (_RAG). Since, the results discussed above showed that the use of Arabic gum worsened the mechanical resistance of BOFD_SD, no improvement would be expected when using the same agglomerative material in its recycled form. Only the mixture BOFD_BFS was then tested with the new binder, hence another batch of BOFD_BFS was prepared.

The solution used in this work was provided by AEB S.p.A. and its chemical composition is reported in Table 3. The new batch was prepared by mixing the raw powders with the recycled Arabic gum, maintaining the solid binder at 5 wt% of the powder weight. The mixture was then dried at 105 °C for 30 min, allowing partial water evaporation and resulting in a final water content of 60.78 wt%. The drying time was not chosen arbitrarily, but defined after several trials at different durations, with the specific aim of obtaining a water/solid ratio as close as possible to that of natural Arabic gum (65.91 wt% moisture and 34.09 wt% solid). Fig. 13 shows an almost linear decrease of the water amount in the solution with time and 30 min has the moisture/solid ratio closer to that of natural Arabic gum (variation about 7 % of the water content of the natural Arabic gum).

The mixture was then compressed to obtain briquettes with the same procedure explained in the Materials and Methods section.

The results of the mechanical characterization of the new briquettes batch are reported in Table 4. The mechanical characterization of BOFD_BFS_RAG is comparable with the results got from BOFD_BFS_AG, confirming the possibility to substitute the natural Arabic gum with a recycled solution without affecting the mechanical resistance of the agglomerates. Both briquettes survived to 10.00 drops, but BOFD_BFS_RAG released fewer fines, with an increase in AIRI and size stability of 41.19 % and 5.97 %, respectively. Conversely, the UCS worsened by around 11.86 % when recycled Arabic gum was used. Despite the reduction in compression resistance, the industrial benchmarks (Adu-Poku et al., 2022; Barisetty et al., 2020) were again satisfied confirming the possibility to substitute the natural Arabic gum with the recycled solution without affecting the mechanical resistance of the agglomerate.

Similarly, the degree of reduction (Table 5) of BOFD_BFS_RAG was not affected by the substitution of the binder in BOFD_BFS_AG showing a variation of −10.42, −0.35 and 1.84 % at 700, 950 and 1200 °C, respectively. The slight discrepancy was attributed to experimental errors (without exceeding the 10 %) and confirmed the self-reduction capacity of the briquettes, regardless of the use of a not natural binder.

The main difference was instead identified in the swelling behavior. BOFD_BFS_AG shrank at all temperatures, while BOFD_BFS_RAG maintained its shape during the reduction at 700 and 950 °C, but swelled at 1200 °C. This is due to the iron whiskers increasing in length in the presence of the recycled binder (Fig. 14b) compared to BOFD_BFS_AG where only nucleation and their thickening were observed (Fig. 14a) (Mantovani et al., 2002).

Since the only difference in the two mixtures was the binder used, both binders were dried for 24 h to remove all moisture. They were then analyzed by SEM to determine the cause of the different swelling behaviors observed. The BSE-SEM images and the spectrum got from SEM-EDS are reported in Fig. 15 and Table 6, respectively.

Both binders were characterized by a matrix which embeds small spots and bigger particles. The SEM analysis identified Si only in the matrix of the recycled Arabic gum, while the natural binder was composed only by carbon and calcium. Similar composition was shown by the white spots present inside both the matrix, respectively. This variation in chemical composition was the main cause for the different swelling behavior of the briquettes (Wang & Sohn, 2011). explained that

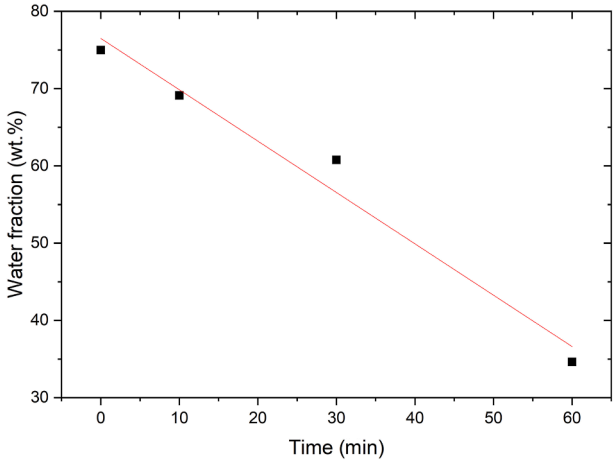

Fig. 13. Water fraction inside the recycled Arabic gum during the drying for different time. (linear regression: y = −0.66x+76.51; R^2 0.97428).

Table 4
Green density, results of drop test and compression test of BOFD_BFS_RAG.

Density (g cm^{-3})	No of drop	IRI	AIRI	Size stability (%)	UCS (MPa)
2.45	10	1000	917.09	98.93	13.98

Table 5
Swelling and degree of reduction at 700, 950 and 1200 °C of BOFD_BFS_RAG.

Temp. (°C)	Swelling (%)	Reduction degree (%)
700	0.99	22.27
950	0.06	36.65
1200	5.60	91.36

Table 3
Chemical composition of recycled Arabic gum expressed in ppm.

Composition	H_2O	COD	Cl^-	F^-	H_2S	N_2	NH_4	PO_4^{3-}	SO_4	Zn
Amount	756000	16800	1110	22.5	40.9	3110	880	970	7800	32

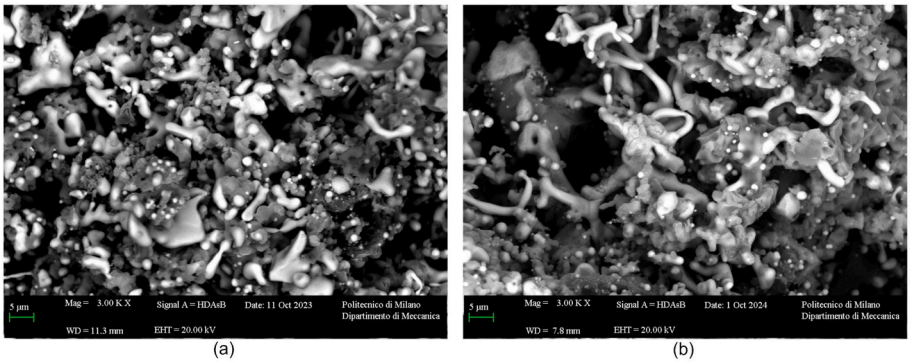

Fig. 14. BSE-SEM images of (a) BOFD_BFS_AG reduced at 1200 °C; (b) BOFD_BFS_RAG reduced at 1200 °C.

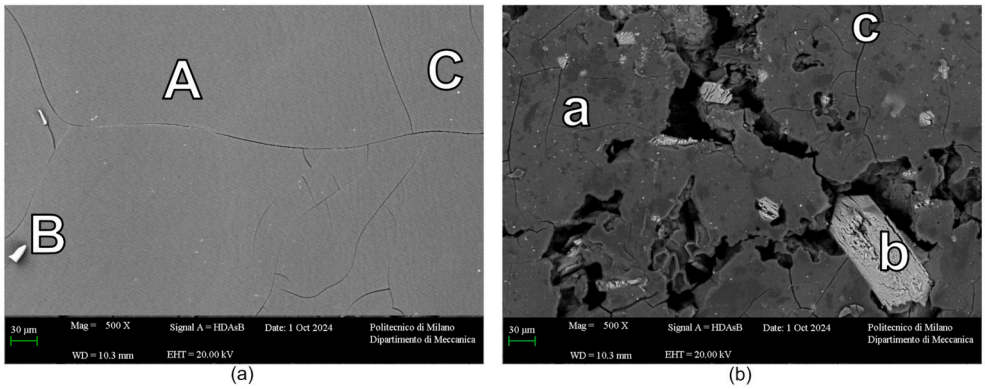

Fig. 15. BSE-SEM of (a) natural Arabic gum dried at 105 °C for 24 h; (b) recycled Arabic gum dried at 105 °C for 24 h.

Table 6
SEM-EDS spectrum of natural (capital letter) and recycled (lowercase letter) Arabic gum expressed in wt.%. ("-" means not detected). "A" and "a" refer to the matrix, "B" and "b" refer to the big white particles and "C" and "c" refer to the small white spots in the matrixes.

Spectrum	C	Ca	Si	S
A	51.64	1.43	–	–
a	47.14	–	9.98	0.02
B	62.51	1.89	–	–
b	22.05	28.79	–	24.12
C	55.73	3.23	–	1.61
c	47.04	–	10.46	0.52

the presence of SiO_2 favored the clustering of long iron whiskers changing their nucleation site distribution. On the contrary, the presence of CaO not only suppressed the iron whiskers growth but promoted larger number of their nucleation and thickening. The same evidence was identified in Fig. 14, where the calcium in the natural Arabic gum favored the nucleation of a high number of thick iron whiskers, while the silicon favored the formation of longer whiskers and consequently an increase in the swelling index. Although the increase in volume, the swelling in BOFD_BFS_RAG was not catastrophic being lower than 20 % (Andersson et al., 2019). The recycled Arabic gum was hence suitable to substitute the natural Arabic gum without affecting the mechanical and metallurgical properties of the briquettes.

4. Conclusion

Integrated cycle steel plant by-products have been agglomerated in pair in form of self-reducing briquettes to recirculate them inside metallurgical processes. The work aimed to verify the suitability of using Arabic gum in metallurgical applications comparing the mechanical and metallurgical properties of the agglomerates. Corn starch-based binder was used as reference. The main conclusions are summarized as follows:

- Arabic gum strengthens fine-particle aggregates (BOFD_BFS) by improving particle packing and densification, but reduces impact resistance in coarse SD aggregates by forming heterogeneous clusters.
- Arabic gum improves particle packing, increasing iron oxide–carbon contact and reduction in fine BFS briquettes; in coarse aggregates, metallurgical performance mainly depends on particle size rather than the binder.
- Arabic gum overcomes the disruptive forces of BOFD_BFS_CS giving self-stand stability to the mixture.
- Arabic gum positively enhances the performance of BOFD_BFS_AG since it survived to 10 drops, had UCS higher than the industrial requirements and degree of reduction higher than 90 % with acceptable metallization.
- It is possible to substitute the natural Arabic gum with a recycled solution without affecting both the mechanical and metallurgical properties of the briquettes.

CRediT authorship contribution statement

Sara Scolari: Writing – review & editing, Writing – original draft, Resources, Investigation, Formal analysis, Data curation, Conceptualization. **Davide Mombelli:** Writing – review & editing, Writing – original draft, Validation, Methodology, Formal analysis, Conceptualization. **Gianluca Dall'Osto:** Writing – review & editing, Validation, Resources, Data curation. **Carlo Mapelli:** Supervision.

Declaration of competing interest

The authors declare that they have no known competing financial interests or personal relationships that could have appeared to influence the work reported in this paper.

Acknowledgments

The authors would like to acknowledge Dr. Marco Rossoni for providing the instrumentation and knowledge necessary to calculate the volume of briquettes after the thermal treatment. The authors would also like to acknowledge AEB S.p.A., in particular, Dr. Matteo Este and Dr. Paolo Machiavelli, for supplying the recycled solution of Arabic gum.

Appendix A. Supplementary data

Supplementary data to this article can be found online at https://doi.org/10.1016/j.partic.2026.01.008.

References

Abdelrahim, A., Aula, M., Iljana, M., Willms, T., Echterhof, T., Steinlechner, S., Mombelli, D., Mapelli, C., Omran, M., Preiss, S., & Fabritius, T. (2022). Suitability of self-reducing and slag-forming briquettes for electric Arc furnace use based on laboratory tests. *Steel Research International, 93*, 1–20.

Adu-Poku, K. A., Appiah, D., Asosega, K. A., Derkyi, N. S. A., Uba, F., Kumi, E. N., Akowuah, E., Akolgo, G. A., & Gyamfi, D. (2022). Characterization of fuel and mechanical properties of charred agricultural wastes: Experimental and statistical studies. *Energy Reports, 8*, 4319–4331. https://doi.org/10.1016/j.egyr.2022.03.015

Alexander, E., Linn, I., & Jacob, L. (2023). *Residual products in the steel industry used for briquetting*.

Alsaqoor, S., Borowski, G., Alahmer, A., & Beithou, N. (2022). Using of adhesives and binders for agglomeration of particle waste resources. *Advances in Science and Technology Research Journal, 16*(3), 124–135. https://doi.org/10.12913/22998624/149456

Andersson, A., Gullberg, A., Kullerstedt, A., Ahmed, H., Sundqvist-Ökvist, L., & Samuelsson, C. (2019). Upgrading of blast furnace sludge and recycling of the low-zinc fraction via cold-bonded briquettes. *Journal of Sustainable Metallurgy, 5*(3), 350–361. https://doi.org/10.1007/s40831-019-00225-x

Apolinar-Valiente, R., Salmon, T., Williams, P., Nigen, M., Sanchez, C., Marchal, R., & Doco, T. (2020). Improvement of the foamability of sparkling base wines by the addition of Acacia gums. *Food Chemistry, 313*, Article 126062. https://doi.org/10.1016/j.foodchem.2019.126062

Barisetty, S., Kalshetty, S., Ramakrishna, S., Vishwanath, S. C., & Balachandran, G. (2020). Cold briquetting of DRI fines for use in steel making process. *Transactions of the Indian Institute of Metals, 73*(2), 449–455. https://doi.org/10.1007/s12666-019-01856-0

Blesa, M. J., Miranda, J. L., Izquierdo, M. T., & Moliner, R. (2003). Curing time effect on mechanical strength of smokeless fuel briquettes. *Fuel Processing Technology, 80*, 155–167.

Borowski, G., Stępniewski, W., & Wójcik-Oliveira, K. (2017). Effect of Starch binder on Charcoal briquette properties. *International Agrophysics, 31*(4), 571–574. https://doi.org/10.1515/intag-2016-0077

Chen, Y., Pei, Z., Feng, D., & Yi, J. (2025). Environmental impact and comprehensive value assessment of epoxy-based binder for asphalt pavement recycling based on LCA and LCC. *Chemical Engineering Journal, 511*, Article 161973. https://doi.org/10.1016/j.cej.2025.161973

Chikamai, B. N., Banks, W. B., Anderson, D. M. W., & Weiping, W. (1996). Processing of gum Arabic and some new opportunities. *Food Hydrocolloids, 10*(3), 309–316.

Dall'Osto, G., Mombelli, D., Scolari, S., & Mapelli, C. (2024). Role of the biogenic carbon physicochemical properties in the manufacturing and industrial transferability of mill scale-based self-reducing briquettes. *Metals, 14*(8), 882. https://doi.org/10.3390/met14080882

Dall'Osto, G., Mombelli, D., Trombetta, V., & Mapelli, C. (2024). Effect of particle size and starch gelatinization on the mechanical and metallurgical performance of Jarosite plus blast furnace sludge self-reducing briquettes. *Journal of Sustainable Metallurgy*. https://doi.org/10.1007/s40831-024-00825-2

Drobíková, K., Plachá, D., Motyka, O., Gabor, R., Kutláková, K. M., Vallová, S., & Seidlerová, J. (2016). Recycling of blast furnace sludge by briquetting with starch binder: Waste gas from thermal treatment utilizable as a fuel. *Waste Management, 48*, 471–477. https://doi.org/10.1016/j.wasman.2015.11.047

Dror, Y., Cohen, Y., & Yerushalmi-Rozen, R. (2006). Structure of gum Arabic in aqueous solution. *Journal of Polymer Science, Part B: Polymer Physics, 44*(22), 3265–3271. https://doi.org/10.1002/polb.20970

Echterhof, T., Willms, T., Preiss, S., Aula, M., Abdelrahim, A., Fabritius, T., Mombelli, D., Mapelli, C., Steinlechner, S., & Unamuno, I. (2019a). Fabrication of agglomerates from secondary raw materials reinforced with paper fibres by stamp pressing process. *Applied Sciences (Switzerland), 9*(19). https://doi.org/10.3390/app9193946

Echterhof, T., Willms, T., Preiß, S., Omran, M., Fabritius, T., Mombelli, D., Mapelli, C., Steinlechner, S., Unamuno, I., Schüler, S., Mudersbach, D., & Griessacher, T. (2019b). Developing a new process to agglomerate secondary raw material fines for recycling in the electric Arc furnace - The Fines2EAF Project. *La Metallurgia Italiana-n, 5*, 31–40.

Ezeakacha, C. P., Rabbani, A., Salehi, S., & Ghalambor, A. (2018). Integrated image processing and computational techniques to characterize Formation damage. *SPE International Conference and Exhibition on Formation Damage Control*. https://doi.org/10.2118/189509-MS

Ezechiel, K., Joel, K. T., Abdon, A., & Roger, D. D. (2022). Accessibility and effects of binder types on the physical and energetic properties of ecological coal. *Heliyon, 8*, Article e11410.

Ferreira, A. C. S., Aguado, R., Carta, A. M. M. S., Bértolo, R., Murtinho, D., & Valente, A. J. M. (2022). Insights into gum Arabic interactions with cellulose: Strengthening effects on tissue paper. *Materials Today Communications, 31*. https://doi.org/10.1016/j.mtcomm.2022.103706

Fuwa, T., & Ba N-Ya, S. (1969). Swelling of iron ore pellets during reduction. *Transactions ISIJ, 9*, 136–146.

Ghosal, S., Indira, T. N., & Bhattacharya, S. (2010). Agglomeration of a model food Powder-GA. *Journal of Food Engineering, 96*, 222–228.

Han, H., Duan, D., & Yuan, P. (2014). Binders and bonding mechanism for RHF briquette made from blast furnace dust. *ISIJ International, 54*(8), 1781–1789. https://doi.org/10.2355/isijinternational.54.1781

Huang, T. Y., Maruoka, D., Murakami, T., & Kasai, E. (2019). Morphology change and carburization characteristic of iron ore-coal composite during reduction under a simulated condition of blast furnace. *ISIJ International, 59*(11), 1982–1990. https://doi.org/10.2355/isijinternational.ISIJINT-2019-178

Jarrar, A. H., Stojanovska, L., Apostolopoulos, V., Feehan, J., Bataineh, M. F., Ismail, L. C., & Al Dhaheri, A. S. (2021). The effect of gum Arabic (Acacia Senegal) on cardiovascular risk factors and gastrointestinal symptoms in adults at risk of Metabolic syndrome: A randomized clinical trial. *Nutrients, 13*(1), 1–10. https://doi.org/10.3390/nu13010194

Koohestani, H., Hasanpoor, J., & Ghasemi, B. (2025). Eco-friendly steelmaking: Exploring the potential of plant-based binder Acacia gum for iron ore pelletizing. *Case Studies in Chemical and Environmental Engineering, 11*, Article 101110. https://doi.org/10.1016/j.cscee.2025.101110

Kopel, Y., & Giovambattista, N. (2019). Comparative stuy of water-meiate interactions between Hyrophilic an hyrophobic nanoscale surfaces. *Journal of Physical Chemistry B, 123*(50), 10814–10824. https://doi.org/10.1021/acs.jpcb.9b08725

Kotta, A. B., Patra, A., Kumar, M., & Karak, S. K. (2019). Effect of molasses binder on the physical and mechanical properties of iron ore pellets. *International Journal of Minerals, Metallurgy and Materials, 26*(1), 41–51. https://doi.org/10.1007/s12613-019-1708-x

Kowitwarangkul, P., Babich, A., & Senk, D. (2014). Reduction Kinetics of Self-Reducing Pellets of Iron Ore. In *American Institute of Science andTechnology Conference Proceeding: (PDF) Determination of the Reaction Rate Controlling Resistance of Goethite Iron Ore Reduction Using CO/CO2 Gases from Wood Charcoal* † (pp. 611–622). Indianapolis, IN, USA. Available from: [accessed Jan 16 2026] https://www.researchgate.net/publication/351228474_Determination_of_the_Reaction_Rate_Controlling_Resistance_of_Goethite_Iron_Ore_Reduction_Using_COCO2_Gases_from_Wood_Charcoal.

Li, Y., Bao, Z., Gu, S., Wang, Z., Zeng, M., He, Z., Chen, Q., Qin, F., & Chen, J. (2026). Effect of molecular weight and protein content on the interfacial activity of soybean soluble polysaccharides. *Food Hydrocolloids, 173*, Article 112180. https://doi.org/10.1016/j.foodhyd.2025.112180

Li, Y., Gan, W., Liu, X., Lin, T., & Huang, B. (2014). Dispersion mechanisms of Arabic gum in the preparation of ultrafine silver powder. *Korean Journal of Chemical Engineering, 31*(8), 1490–1495. https://doi.org/10.1007/s11814-014-0069-4

Li, Y., Wei, H., Khan, I. U., Omran, M., Fabritius, T., Shu, Q., Wang, C., & Zang, Y. Y. Y. (2023). Reduction kinetics of cold-bonded briquette prepared from return fines of sinter with carbon monoxide and coke. *Steel Research International*, 1–14.

Liu, C., & Chen, J. (2022). High temperature degradation mechanism of concrete with plastering layer. *Materials, 15*(2), 398. https://doi.org/10.3390/ma15020398

Lohmeier, L., Thaler, C., Harris, C., Wollenberg, R., & Schröder, H.-W. (2020). Briquetting of fine-grained residues from iron and steel production using organic and inorganic binders. *Steel Research International, 91*(12). https://doi.org/10.1002/srin.202000238

Lund, D., & Lorenz, K. J. (1984). Influence of time, temperature, moisture, ingredients, and processing conditions on starch gelatinization. *CRC Critical Reviews in Food Science & Nutrition, 20*(4), 249–273. https://doi.org/10.1080/10408398409527391

Ma, Y., Li, Q., Chen, X., Zhang, Y., Yang, Y., & Zhong, Q. (2024). Reducing bentonite usage in iron ore pelletization through a novel polymer-type binder: Impact on pellet induration and metallurgical properties. *Journal of Materials Research and Technology, 30*, 8019–8029. https://doi.org/10.1016/j.jmrt.2024.05.175

Mantovani, M. C., & Takano, C. (2000). The strength and the high temperature behaviors of self-reducing pellets containing EAF dust. *ISIJ International, 40*(3), 224–230.

Mantovani, M. C., Takano, C., & Büchler, P. M. (2002). Electric arc furnace dust-coal composite pellet: Effects of pellet size, dust composition, and additives on swelling and zinc removal. *Ironmaking and Steelmaking, 29*(4), 257–265. https://doi.org/10.1179/030192302225004494

Mombelli, D., Di Cecca, C., Mapelli, C., Barella, S., & Bondi, E. (2016). Experimental analysis on the use of BF-sludge for the reduction of BOF-Powders to Direct Reduced Iron (DRI) production. *Process Safety and Environmental Protection, 102*, 410–420. https://doi.org/10.1016/j.psep.2016.04.017

Mombelli, D., Gonçalves, D. L., Mapelli, C., Barella, S., & Gruttadauria, A. (2021). Processing and characterization of self-reducing briquettes made of Jarosite and blast furnace sludges. *Journal of Sustainable Metallurgy, 7*(4), 1603–1626. https://doi.org/10.1007/s40831-021-00419-2

Mothe Â, C. G., & Rao, M. A. (2000). Thermal behavior of gum Arabic in comparison with cashew gum. *Thermochimica Acta*, 9–13.
Nigen, M., Valiente, R. A., Iturmendi, N., Williams, P., Doco, T., Moine, V., Massot, A., Jaouen, I., & Sanchez, C. (2019). The colloidal stabilization of young red wine by Acacia Senegal gum: The involvement of the protein backbone from the protein-rich arabinogalactan-proteins. *Food Hydrocolloids, 97*, Article 105176. https://doi.org/10.1016/j.foodhyd.2019.105176
Okegbile, O., Baba Hassan, A., Okegbile, O. J., Hassan, A. B., Mohammed, A., & Irekeola, B. J. (2014). Effect of starch and gum Arabic binders in the combustion characteristics of Briquette prepared from sawdust. *Article in International Journal of Scientific and Engineering Research, 5*(3). http://www.ijser.org.
Olugbade, T., Ojo, O., & Mohammed, T. (2019). Influence of binders on combustion properties of biomass briquettes: A recent review. In *Bioenergy research*. New York: Springer. https://doi.org/10.1007/s12155-019-09973-w. LLC.
Omoniyi, T. E., & Igbo, P. K. (2016). Physico-mechanical characteristics of rice husk briquettes using different binders. *Agric Eng Int: CIGR Journal, 18*(1), 70–81.
Önal, M., & Sarıkaya, Y. (2007). Thermal behavior of a bentonite. *Journal of Thermal Analysis and Calorimetry, 90*(1), 167–172. https://doi.org/10.1007/s10973-005-7799-9
Patil, D. P., Taulbee, D., Parekh, B. K., & Honaker, R. (2009). Briquetting of coal fines and sawdust - Effect of particle-size distribution. *International Journal of Coal Preparation and Utilization, 29*(5), 251–264. https://doi.org/10.1080/19392690903294423
Philippe, B. H., Lat, G. N., Alfredo, N., & Diouma, K. (2018). Physicochemical and mechanical properties of biomass coal briquettes produced by artisanal method. *African Journal of Environmental Science and Technology, 12*(12), 480–486. https://doi.org/10.5897/ajest2018.2568
Prasad, N., Thombare, N., Sharma, S. C., & Kumar, S. (2022). Gum arabic – A versatile natural gum: A review on production, processing, properties and applications. In *Industrial crops and products* (Vol. 187)Elsevier B.V. https://doi.org/10.1016/j.indcrop.2022.115304.
Rabbani, A., & Salehi, S. (2017). Dynamic modeling of the formation damage and mud cake deposition using filtration theories coupled with SEM image processing. *Journal of Natural Gas Science and Engineering, 42*, 157–168. https://doi.org/10.1016/j.jngse.2017.02.047
Sanchez, C., Nigen, M., Mejia Tamayo, V., Doco, T., Williams, P., Amine, C., & Renard, D. (2018). Acacia gum: History of the future. *Food Hydrocolloids, 78*, 140–160. https://doi.org/10.1016/j.foodhyd.2017.04.008
Sandhu, K., & Singh, N. (2007). Some properties of corn starches II: Physicochemical, gelatinization, retrogradation, pasting and gel textural properties. *Food Chemistry, 101*(4), 1499–1507. https://doi.org/10.1016/j.foodchem.2006.01.060
Schirmer, M., Jekle, M., & Becker, T. (2015). Starch gelatinization and its complexity for analysis. *Starch/Starke, 67*, 30–41.
Scolari, S., Dall'Osto, G., Tuveri, A., Mombelli, D., & Mapelli, C. (2025). Optimization of red mud and blast furnace sludge self-reducing briquettes propaedeutic for subsequent magnetic separation. *Metals, 15*(10), 1108. https://doi.org/10.3390/met15101108
Scolari, S., Mombelli, D., Dall'Osto, G., & Mapelli, C. (2025). Effect of water-powder interaction on the mechanical and metallurgical behavior of integrated steel plant byproducts agglomerates. *Particuology, 105*, 74–87. https://doi.org/10.1016/j.partic.2025.07.019
Seetharaman, S. (2013). *Treatise on Process Metallurgy (Industrial Processes* (3).
Sen, R., Wiwatpanyaporn, S., & Annachhatre, A. P. (2016). Influence of binders on physical properties of fuel briquettes produced from cassava Rhizome waste. *International Journal of Environment and Waste Management, 17*(Issue 2).
Singh, M., & Bjorkman, B. (2004a). Effect of processing parameters on the swelling behaviour of cement-bonded briquettes. *ISIJ International, 44*(1), 59–68.
Singh, M., & Bjorkman, B. (2004b). Effect of reduction conditions on the swelling behaviour of cement-bonded briquettes. *ISIJ International, 44*(2), 294–303.
Sivrikaya, O., & Arol, A.İ. (2012). The bonding/strengthening mechanism of colemanite added organic binders in iron ore pelletization. *International Journal of Mineral Processing, 110–111*, 90–100. https://doi.org/10.1016/j.minpro.2012.04.010
Sotannde, O. A., Oluyege, A. O., & Abah, G. B. (2012). Physical and combustion properties of charcoal briquettes from neem wood residues. *International Agrophysics, 24*, 189–194.
Strezov, V., Lucas, J. A., & Wall, T. F. (2005). Effect of pressure on the swelling of density separated coal particles. *Fuel, 84*(10), 1238–1245. https://doi.org/10.1016/j.fuel.2004.06.035
Trpčevská, J., Piroskova, J., & Pribulova, A. (2015). Alternative binding materials for the briquettes production from the metallurgical wastes hard zinc processing, production of alloys from zinc drosses view Project. *Metall, 69*, 133–138. https://www.researchgate.net/publication/282307792.
Wang, S., Li, C., Copeland, L., Niu, Q., & Wang, S. (2015). Starch retrogradation: A comprehensive review. *Comprehensive Reviews in Food Science and Food Safety, 14*, 568–581.
Wang, H. T., & Sohn, H. Y. (2011). Effect of CaO and SiO2 on swelling and iron whisker Formation during reduction of iron oxide compact. *Ironmaking and Steelmaking, 38*(6), 447–452. https://doi.org/10.1179/1743281211Y.0000000022
Wu, W., Meng, H., Liu, L., Yuan, T., Bai, Y., & Yan, Z. (2012). Slag melting characteristic of slag forming and slag splashing for BOF less slag smelting. *Journal of Iron and Steel Research International, 19*(7), 20–25. https://doi.org/10.1016/S1006-706X(12)60108-3
Yahaya, D. B., & Ibrahim, T. G. (2012). Development of rice husk briquettes for use as fuel. *Research Journal in Engineering and Applied Sciences, 1*(2), 130–133. www.emergingresource.org.
Zhang, G., Sun, Y., & Xu, Y. (2018). Review of briquette binders and briquetting mechanism. In *Renewable and sustainable energy reviews* (Vol. 82, pp. 477–487). Elsevier Ltd. https://doi.org/10.1016/j.rser.2017.09.072.
Zhao, Z., Tang, H., & Guo, Z. (2013). Effects of CaO on precipitation morphology of metallic iron in reduction of iron oxides under CO atmosphere. *Journal of Iron and Steel Research International, 20*(7), 16–24. https://doi.org/10.1016/S1006-706X(13)60120-X